Catalysis Letters, Vol. 117, Nos. 3–4, September 2007 (© 2007)
DOI: 10.1007/s10562-007-9116-7

$CuO–CeO_2/Al_2O_3$ /FeCrAl monolithic catalysts prepared by sol-pyrolysis method for preferential oxidation of carbon monoxide

S. H. Zeng,[a] Y. Liu,[a,*] and Y. Q. Wang[b]

[a]*Department of Catalysis Science and Technology, School of Chemical Engineering and Technology, Tianjin University, Tianjin, 300072, P. R. China*
[b]*Key Laboratory of Green Chemical Technology, School of Chemical Engineering and Technology, Tianjin University, Tianjin, 300072, P. R. China*

Received 24 March 2007; accepted 3 April 2007

This work describes a new technique, sol-pyrolysis method, for depositing CuO–CeO_2on FeCrAl honeycomb supports. The monolithic catalysts prepared by the method presented good adhesion stability in ultrasonic and thermal shock tests. The principle of the deposition and the role of the support were studied and analyzed by SEM, XRD, TG-DTA, TPR and XPS techniques. The results showed that the active components adhered to the support via three stages. High surface energy of the crystal nuclei and the interaction between the active components and the support promoted adhesion stability. Moreover, the presence of the support influenced distribution and interaction of the active components, but had no obvious effect on catalytic performance. The CuO–CeO_2/Al_2O_3/FeCrAl monolithic catalysts were applied for the preferential oxidation of carbon monoxide in rich-hydrogen gases and revealed high activity and good selectivity under the presence of 15%CO_2 and 10%H_2O.

KEY WORDS: monolith; CuO; CeO_2; FeCrAl; pyrolysis; hydrogen; preferential oxidation.

1. Introduction

Proton exchange membrane fuel cells (PEMFC), which use high purity hydrogen as energy source, are becoming an increasingly attractive technology for power generation because of their high-energy conversion efficiency and nearly zero emission [1,2]. The conventional method of hydrogen production combines catalytic steam reforming with water gas shift reaction and the resulting streams contain approximately 50% H_2, 15% CO_2, 10% H_2O, 25% N_2, and 0.5–1% CO [3–6]. However, the inlet gas feed for the PEMFC requires very low CO concentration to avoid poisoning the Pt electrodes. Therefore, it is necessary to reduce CO concentration leaving the water–gas-shift (WGS) reactor from 1% to less than 10 ppm in the presence of steam, CO_2, and high H_2 concentration [5–10].

Preferential oxidation of CO is regarded as a favorable method for the purification of the rich-hydrogen streams due to its efficiency and simplicity. So far, various catalysts have been studied for the preferential CO oxidation, from base metals like Cu and Co, to noble metals such as Pt, Pd, Ru and Au [2–9]. Supported noble metals are efficient catalysts for the preferential CO oxidation. Due to the limited availability of precious metals, much attention has been given to the base metal catalysts. CuO–CeO_2 catalysts were found to be highly active and selective for the preferential oxidation of CO [3,4].

*To whom correspondence should be addressed.
E-mail: yuanliu@tju.edu.cn

Recently monoliths have received attention as supports for PROX catalysts [1,10–12]. The macrostructure of the support material ensures a low-pressure drop, whereas the thin catalytic coating ensures high efficiency and selectivity [10–18]. Although monoliths are widely used in exhaust gas cleaning, their application in PROX catalytic process is in developing stage and only few papers are published [1,10–12,19].

Adhesion stability is a very important property for the monolithic catalysts. It directly influences the use and efficiency of the monoliths during the operation [1,11–18]. FeCrAl metallic monoliths present some advantages over cordierite ceramic monoliths such as higher thermal conductivity, lower heat capacity and greater thermal and mechanical shock resistance [1,20–22]. However, adhesion on the metallic monoliths has not been as well developed yet as that on the ceramic monoliths [20–22]. The conventional methods for the deposition of catalysts on FeCrAl substrates include impregnation and dip-coating. These two kinds of methods are simple, but adhesion stability is difficult to reach the request.

In this work, an alternative method for depositing CuO–CeO_2 on FeCrAl substrates is presented. It produces a well-adherent layer of CuO–CeO_2 directly on FeCrAl honeycombs by using a sol-pyrolysis process. This process is easy to operate and only needs simple instrument. It was found that the CuO–CeO_2/Al_2O_3/FeCrAl monolithic catalysts prepared by the sol-pyrolysis exhibited good catalytic activity for PROX.

2. Experimental

2.1. Catalyst preparation

Heat-resistant FeCrAl honeycombs with cell densities of 400 cells per square inch were chosen as the metallic supports. The wall thickness, length and diameter of the honeycombs monolith were 0.04, 15 and 7 mm, respectively. The chemical composition of the FeCrAl alloy was as follows: C 0.035, Si 0.5, Mn 0.5, P 0.018, S 0.015, Ni 0.5, Ce 0.2, Cr 20.5, Al 5.0, Fe balance. Before starting the coating procedure all the supports were washed with acetone in an ultrasonic bath for 30 min to remove the superficial impurities, and then rinsed with de-ionized water. The metallic supports were put into the 60 °C NaOH solution for 10 min and rinsed with de-ionized water. Furthermore, the supports were pretreated in the H_3PO_4 and HNO_3 (3: 1 molar ratio) acid solution at 85 °C for 15 min, followed by rinsing with de-ionized water. Finally, the metallic supports were heated from room temperature to 950 °C with heating rate 5 °C /min and oxidized at 950 °C for 5 h in a muffle, and then cooled to room temperature.

The $CuO–CeO_2/Al_2O_3$/FeCrAl monolithic catalysts were prepared according to the following procedure: (1) $Cu(NO_3)_2$, $Ce(NO_3)_3$ and citric acid were dissolved in 90 ml de-ionized water in the appropriate amounts to obtain solutions with the following characteristics: 1 M in total metals; Cu/(Cu + Ce) molar ratio = 0.15; citric acid/(Cu + Ce) molar ratio = 0.8, 1.0, 1.2 or 1.4. (2) The solutions were left at 70 °C for 6 h to change into a sol [23,24]. (3)The supports after the pretreatment were heated to 550 °C or 600 °C for 10 minutes and inserted into the sol. (4) After 10 s, the supports were taken out, dried and calcined at a certain heating rate to 550 °C or 600 °C. (5) Steps 3–4 were repeated until about 0.04 g/cm^3 catalyst loading was achieved.

The particle catalyst of $CuO–CeO_2$ was prepared by drying and calcining the sol made by step 1 and 2.

The preparation conditions of the monolithic catalysts were listed in table 1.

2.2. Adhesion tests

Adhesion properties of the catalysts on the substrate surface were determined qualitatively using an ultrasonic adhesion test and a thermal shock test. The catalysts were immersed in petroleum ether inside a sealed beaker, and then treated in a 40 KHz/100 W ultrasonic bath for 30 min to measure the weight loss caused by exposure to the ultrasonication. The thermal shock test was carried out by heating the catalysts to 800 °C and kept at this temperature for 20 min, and then quenched in water at 25 °C. This thermal shock process was repeated 10 times for each sample, after which the weight loss was measured.

2.3. Catalyst characterization

The textural structure of the monoliths was analyzed by a scanning electron microscope (PHILIPS XL 30 ESEM) with energy dispersive X-ray detector (EDX).

TG-DTA curves were measured on a thermal analysis device (PerkinElmer). Approximate 30 mg sample was heated at a rate of 10 °C /min in an air stream of 100 ml/min, using α-alumina as reference.

X-ray diffraction (XRD) patterns of the samples were recorded on a Philip X'pert Pro diffractometer. Cobalt Kα radiation (λ = 0.178901 nm) was used with a power setting of 40 kV and 40 mA.

TPR was carried on a Thermo-Finnigan instrument in the 5% H_2/Ar gas mixture. The flowrate of the gas was 30 ml/min and the heating rate is 10 °C /min.

X-ray photoelectron spectroscopy (XPS) spectra were recorded on an PHI1600ESCA SYSTEM Spectrometer with Mg Kα radiation (1253.6 eV). C 1s line at 284.6 eV was used as an internal standard for correction of binding energies.

2.4. Catalytic performance tests

The catalytic oxidation of CO in rich-hydrogen gases was carried in a quartz reactor inserted in a vertical furnace. The reaction mixture consisted of 1%CO, 1%O_2,

Table 1
Preparation conditions and weight loss of the $CuO–CeO_2/Al_2O_3$/FeCrAl monolithic catalysts

Sample number	Citric acid/(Cu + Ce)	Decomposing and calcination temperature (°C)	Heating rate (°C/min)	Coating time	Weight loss (%)	
					Ultrasonic	Thermal shock
$CuO–CeO_2$-1	0.8	600	5	5	15.38	11.11
$CuO–CeO_2$-2	1.0	600	5	5	8.00	5.40
$CuO–CeO_2$-3	1.2	600	5	4	10.34	10
$CuO–CeO_2$-4	1.4	600	5	4	13.88	9.09
$CuO–CeO_2$-5	1.0	600	10	5	17.64	14.70
$CuO–CeO_2$-6	1.0	550	5	5	8.82	5.88
$CuO–CeO_2$-7	1.0	550	1	5	8.57	8.82
$CuO–CeO_2$ particle	1.0	600	5	–	–	–

15%CO_2, 10%H_2O and 50%H_2 (volume fraction) with N_2 as balance gas. H_2O was fed with a syringe pump, passing through an evaporator, into the reactor. The space velocity was 40,000 ml $\cdot$ g_{cat}^{-1} $\cdot$ h^{-1}. The reaction was operated between 100 °C and 225 °C. The bed temperature was measured by means of a thermocouple inserted in the furnace. Product and reactant analyses were conducted by a SP-3420 gas chromatograph. 5A molecular sieve column was used to separate CO, O_2 and N_2 . CO_2 was determined by GDX-502 column. Water was trapped before the gases entering the GC. $CO_2$was absorbed before entering 5A molecular sieve.

The conversion of CO (C_{CO}) and the selectivity for CO oxidation (S_{CO}) were calculated according to equation (1) and (2):

$$C_{CO} = \frac{\text{inletCOconcentration} - \text{outletCOconcentration}}{\text{inletCOconecntration}} \times 100\% \quad (1)$$

$$S_{CO} = \frac{\text{inletCOconcentration} - \text{outletCOconcentration}}{2 \times (\text{inlet}O_2\text{concentration} - \text{outlet}O_2\text{contration})} \times 100\% \quad (2)$$

3. Results

3.1. Adhesion stability

Table 1 lists the adhesion stability of the samples prepared in this work via ultrasonic and thermal shock tests. The monolithic catalysts exhibit good adhesion stability. In particular, the weight losses of the CuO–CeO_2-2 monolithic catalyst in ultrasonic and thermal shock are 8.00% and 5.4%, respectively, showing the best adhesion stability among the monolithic catalysts tested. It is obvious that preparation conditions have effect on the adhesion stability. This will be discussed later.

3.2. Textural features

Figure 1 reveals the surface features of the FeCrAl substrate after pretreatment. It can be seen that the surface of the support becomes very course. The result of EDX shows that the surface consists of 38.21 % O, 30.58 % Al, 9.38 % Cr and 21.83 % Fe in weight, indicating that the alumina is formed on the surface of support. XRD result in figure 4 shows that this layer alumina includes α–Al_2O_3 as well as γ–Al_2O_3. The formation of alumina enhances the specific surface area of the support and acts as a host for the metal oxides. On the other hand, compared to FeCrAl support, the thermal expansion coefficient of the alumina is much closer to those of the metal oxides, hence the metal oxides interacted with the alumina layer should exhibit good adhesion stability [11–18]. As exhibited in figure 2, the CuO–CeO_2 catalyst is compactly and homogeneously distributed on the substrate.

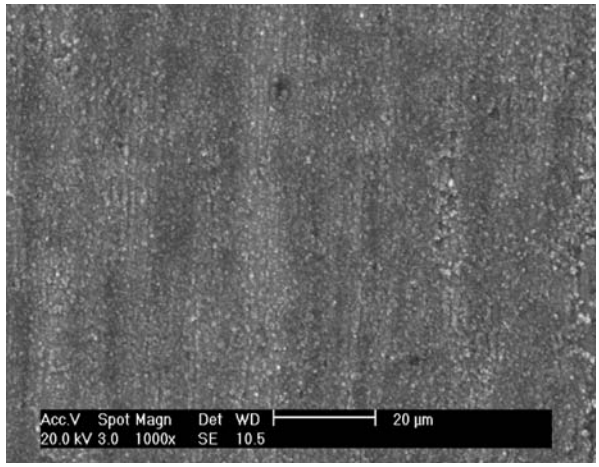

Figure 1. SEM of the FeCrAl support after the pretreatment.

3.3. TG-DTA measurements

Figure 3 shows TG-DTA curves of the CuO–CeO_2-2 monolithic catalyst. On the curve of DTA, the exothermic peak of 134 °C corresponds to the decomposition of nitric acid. The exothermic peaks at 280 °C are attributed to decomposition and combustion of the metal citrates. The DTA peaks are accordant with the weight losses of two steps on the curve of TG. According to the data of TG, the molar ratio of citric acid/(Cu + Ce) equals to 0.85 on the FeCrAl substrate. However, the ratio is 1 in the colloid solution. It means that a part of the metal citrates in the sol decomposed into CuO and CeO_2 as soon as metal substrate was rapidly put into the colloid solution. The calculation result shows that about 15.5% loading of CuO and CeO_2 is achieved via rapid decomposition of the metal

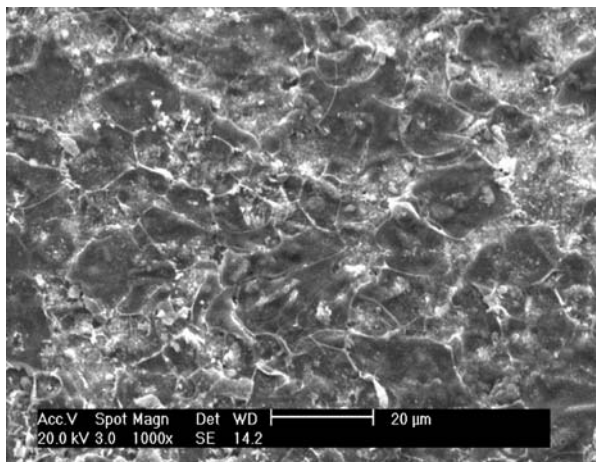

Figure 2. SEM of the CuO–CeO_2-2 monolithic catalyst.

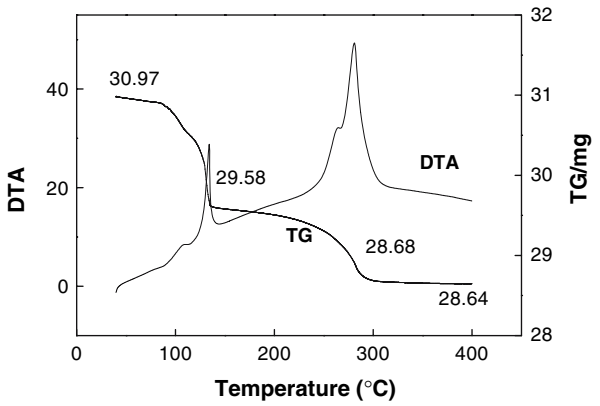

Figure 3. TG-DTA curves of the CuO–CeO_2 −2 monolithic catalyst.

citrates into CuO and CeO_2 in the dipping process (step 3 in the catalyst preparation), and 84.5% loading of CuO and CeO_2 is achieved through the decomposition of the metal citrates in the course of calcination. The details are discussed in section 4.1.

3.4. XRD measurements

Figure 4 shows the XRD spectra of the samples prepared in this work. The diffraction peaks of FeCr, α–Al_2O_3 and γ–Al_2O_3 are presented on the FeCrAl support after pretreatment. In the spectrum of CuO–CeO_2 particle catalyst, the diffraction peaks of only CeO_2 can be observed. The diffraction peaks of CuO, CeO_2, FeCr, α–Al_2O_3 and γ–Al_2O_3 appear in the spectra of the monolithic catalysts. The detail is listed in table 2. Compared with the particle catalyst, the diffraction peaks of CeO_2 become broader and the diffraction peak of CuO appears in monolithic catalysts. At the same time, the diffraction peaks of Al_2O_3 become weaker, broader and even disappear in the monolithic catalysts compared with the pretreated support.

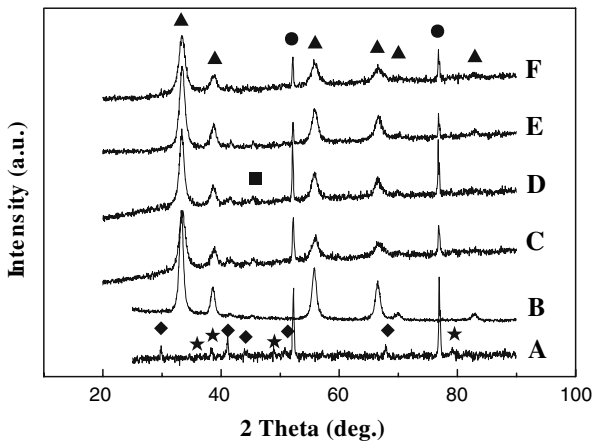

Figure 4. XRD patterns of (A) FeCrAl support after pretreatment, (B) CuO–CeO_2 particle, (C) CuO–CeO_2-1, (D) CuO–CeO_2-2, (E) CuO–CeO_2-3 and (F) CuO–CeO_2-4. (▲) CeO_2; (●) FeCr; (■) CuO; (◆) α-Al_2O_3; (★) γ-Al_2O_3

3.5. TPR measurements

The H_2-TPR profiles of the catalysts are presented in Figure 5. Pure CuO has only one reductive peak at 330 °C. Pure ceria is reduced at 480 °C and 750 °C, which are attributed to the reduction of the surface ceria and bulk ceria, respectively [2,4,7,25].

There are four peaks on the TPR profile of the CuO–CeO_2 particle catalyst. The strong peaks of 200 °C and 260 °C correspond to the reduction of highly dispersed copper species, which interacts with ceria and is the key active component [2,4,7,25]. The peaks of 480 °C and 850 °C are attributed to the reduction of the surface and bulk ceria, respectively.

In the profile of the CuO–CeO_2-2 monolithic catalyst, there are five reductive peaks, which appear at 200 °C, 260 °C, 340 °C, 550 °C and 720 °C, respectively. As shown in figure 5, the five reductive peaks are named as α_1, α_2,α_3,β and γ. Similarly, α_1 and α_2 are attributed to the reduction of highly dispersed copper species. The α_3 peak corresponds to the reduction of bulk CuO particles, indicating that copper oxide tends to aggregate on the surface of FeCrAl substrate. The peaks of 550 °C and 720 °C are attributed to the reduction of surface and bulk ceria, respectively.

3.6. XPS measurements

XPS measurements show that the shape and binding energy of Cu 2p, Ce 3d, and O 1s peaks have no much difference between the particle and monolithic catalysts, indicating that chemical states of the surface components do not change appreciably when the particle catalyst is loaded on the FeCrAl substrate.

The surface compositions (Cu/(Cu + Ce) atom ratio) are estimated by XPS. The values are 0.451 and 0.406 for the particle and the monolithic catalyst, respectively. It is clear that these values are nearly three times than the nominal compositions (0.15) of the samples, suggesting that copper species enriches on the surface of the catalysts for both the monolithic and the particle catalyst. Similar phenomenon was also reported in literatures [5–7].

3.7. Catalytic performance tests

Figure 6 compares CO conversion and selectivity for PROX over the particle and monolithic catalysts. As shown in figure 6, both of the particle and monolithic catalysts exhibit high activity for CO oxidation in rich-hydrogen rich gases. They attain 100% CO conversion with 53% selectivity at 165 °C under the presence of 15% CO_2 and 10% H_2O. The operational window of total conversion is from 165 °C to 185 °C. The results suggest that the catalytic performance of the CuO–CeO_2/Al_2O_3/FeCrAl monolithic catalyst is as good as the particle catalyst after isometric particle catalyst is loaded on the FeCrAl support.

Table 2
Characterization results of the catalysts

Sample	XRD phases	d_{CeO2} (nm)	BET (m^2/g)	XPS Cu/(Cu + Ce)
CeO_2	CeO_2	14.1		
FeCrAl after pretreatment	FeCr,α–Al_2O_3,γ–Al_2O_3			
$CuO–CeO_2$-1	CeO_2,CuO,FeCr, α–Al_2O_3, γ–Al_2O_3	6.7		
$CuO–CeO_2$-2	CeO_2,CuO,FeCr, α–Al_2O_3, γ–Al_2O_3	9.0	4.69	0.406
$CuO–CeO_2$-3	CeO_2,CuO,FeCr, α–AL_2O_3, γ–Al_2O_3	8.1		
$CuO–CeO_2$-4	CeO_2,CuO,FeCr, α–AL_2O_3, γ–Al_2O_3	7.5		
$CuO–CeO_2$ particle	CeO_2	11.5	25.29	0.451

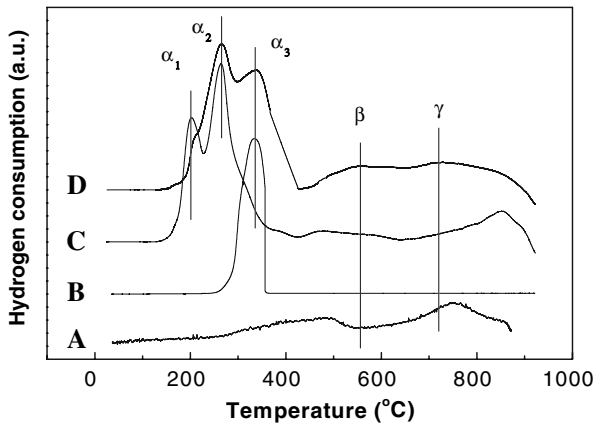

Figure 5. TPR profiles of the particle and monolithic catalysts: (A) CeO_2; (B) CuO; (C) $CuO–CeO_2$ particle; (D) $CuO–CeO_2$-2 monolith.

The performance of the monolithic catalyst and the particle catalyst is nearly the same, as shown in figure 6, which may result from the integrated impact of reverse water gas shift reaction, heat and mass transfer. Firstly, CO oxidation is a fast and exothermic reaction, while the reverse water gas shift is an endothermic reaction. The presence of hot spots in the particle catalyst degrades the catalytic performance by activating the reverse water gas shift reaction and decreasing the net CO conversion [19]. On the other hand, FeCrAl support is beneficial for heat transfer and temperature homogeneity, which weakens the unfavorable effect of the reverse water gas shift reaction on CO preferential oxidation. Secondly, the TPR and XRD results show that the content of the highly dispersed CuO becomes lower when $CuO–CeO_2$ is loaded on the monolith, which may reduce the catalytic activity because highly dispersed CuO is the active component for CO oxidation [2,4,7,25]. Thirdly, the effect of mass transfer on the catalytic performance is a rather complicated subject for comparing the monolith with the particle packed-bed catalyst. Zinnias [11] found that no external mass transfer limitations occurred on the Pt/Al_2O_3 monolith catalyst, different from their packed-bed catalyst, and limitations may arise from internal diffusion within the porous catalyst itself. The reason why the present monolithic and the particle catalysts have the same performance in the CO preferential oxidation reaction needs to be studied further.

The durability of the monolithic catalyst was tested, as shown in figure 7. The $CuO–CeO_2$-2 monolithic catalyst maintains 100% CO conversion at 165 °C for 50 operation hours. The catalytic performance results of figures 6 and 7 show that it is promising for using the $CuO–CeO_2/Al_2O_3$/FeCrAl monolithic catalysts pre-

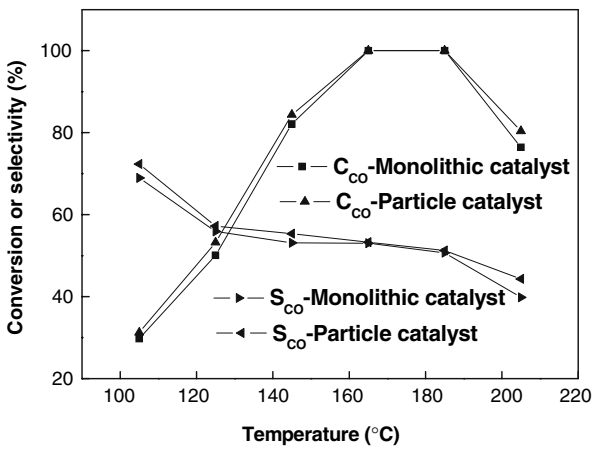

Figure 6. CO conversion and selectivity over the particle and monolithic catalysts ([CO]in = 1%; $[O_2]$in = 1%; $[CO_2]$in = 15%; $[H_2O]$in = 10%; $[H_2]$in = 50%; N_2 balance).

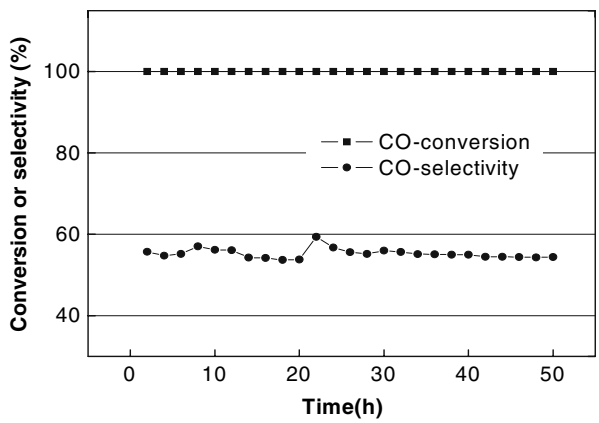

Figure 7. CO conversion and selectivity over the $CuO–CeO_2$-2 monolithic catalyst for 50 h ([CO]in = 1%; $[O_2]$in = 1%; $[CO_2]$in = 15%; $[H_2O]$in = 10%; $[H_2]$in = 50%; N_2 balance).

pared by the sol-pyrolysis method for the preferential oxidation of CO in H_2 rich gases.

4. Discussion

4.1. Analysis of adhesion stability

For the sol-pyrolysis method, the metal substrates are heated to the temperature of higher than the decomposition temperature of the metal citrates, and then rapidly inserted into the colloid solution. The coating process of the active components on the supports may divide into the following three stages: (1) When the temperature of the supports are higher than the decomposition temperature of the metal citrates, the metal citrates immediately decompose into minute crystal nuclei of CuO and CeO_2 on the hot contact surface between colloid solution and the supports. At this moment, the crystal nuclei possess high surface energy, and incline to form chemical bond with the alumina on the support surface and tightly adhere to the supports. (2) After the first stage, the temperature of the supports drops. As shown in figure 3, the temperature of dehydration of the metal citrates is higher than 134 °C, and the decomposition temperature of the metal citrates is about 280 °C. When the temperature of the supports is between 134 °C and 280 °C, the crystal nuclei of the metal citrates would dehydrate and separate out from the colloid solution. Similarly, the crystal nuclei of the citrates also hold high surface energy and tightly adhere to the surface of supports. (3) When the temperature further drops to lower level, some colloid particles of the metal citrates directly adhere to the surface of the supports via Van der Waals force. The crystal nuclei and colloid particles of the metal citrates, from stages 2 and 3, will decompose into CuO and CeO_2 in the calcination process, as stated in section 3.3. The monoliths are coated 4–5 times. In the coating process, the monoliths are heated to 550 or 600 °C and inserted into the colloid solution again and again, so the loose particles drop from the surface during the preparation course. Consequently, CuO and CeO_2 tightly adhere to the supports.

Alumina crystal clusters grow out from the FeCrAl substrates, so they tightly integrate with the substrates. XRD analysis shows that the diffraction peaks of Al_2O_3 and CeO_2 become weaker and broader in the $CuO–CeO_2/Al_2O_3$/FeCrAl monolithic catalysts, indicating that chemical bonds are formed between CeO_2 and Al_2O_3 particles, that is, the interface between CeO_2 and the alumina particles is linked by chemical bonds. The catalyst components connect with the support via chemical bond, so they are combined very tightly.

Above all, high surface energy of the small crystal nuclei and interaction between the active components and the support promote the adhesion stability of the monolithic catalysts, hence the $CuO–CeO_2/Al_2O_3$/FeCrAl monolithic catalysts exhibit high adhesion stability.

4.2. The effect of support on the structure of $CuO–CeO_2$ catalyst

The crystallite sizes are estimated by applying Scherrer's equation to the CeO_2 peaks of the XRD spectra [5]. From table 2, it is clear that the CeO_2 crystallite sizes on FeCrAl substrate become smaller than that in the particle catalyst. As mentioned above, CeO_2 and Al_2O_3 react on the surface of mutual contact. The interaction between CeO_2 and Al_2O_3 promotes CeO_2 to highly disperse on the surface of the support, so CeO_2 crystallite sizes become smaller. TPR study shows that the reduction temperature of the surface ceria increases in the profile of the $CuO–CeO_2/Al_2O_3$/FeCrAl monolithic catalyst, compared with the particle catalyst, indicating that the interaction between CeO_2 and Al_2O_3 affects the reduction of surface ceria.

XRD results show that the diffraction peak of copper oxide can not be observed in the spectrum of the $CuO–CeO_2$ particle catalyst, while weak diffraction peak of CuO appears in the spectra of the $CuO–CeO_2/Al_2O_3$/FeCrAl monolithic catalysts. Similarly, the reductive peak of the bulk CuO is obviously stronger in the TPR profile of the monolithic catalyst than that in the particle catalyst. These results suggest that CuO tends to aggregate on the surface of the FeCrAl substrate. In addition, XPS analysis shows that the chemical states of the surface components do not change appreciably when the particle catalyst is loaded on the FeCrAl substrate, namely highly dispersed copper oxide still enrich on the outside surface of the catalyst though partial CuO aggregates in the monolithic catalyst. In PROX reaction, a small quantity of highly dispersed copper oxide, about 5∼8wt% in $CuO–CeO_2$ catalyst, is enough for keeping the high activity, and increasing the copper content to higher value does not increase the activity further [3, 4]. The highly dispersed CuO amounts to about 8wt% in the $CuO–CeO_2$-2 monolithic catalyst, deduced from the hydrogen consumption of TPR and the total CuO content in the catalyst. Thus it is speculated that the catalytic activity of the monolithic catalyst is not markedly affected by the aggregation of partial copper oxide on the substrate.

4.3. The influence of coating conditions on adhesion stability

The results of table 1 show that the molar ratio of citric acid/(Cu + Ce) and the heating rate influence the adhesion stability of the active components on the support. Different molar ratios of citric acid/(Cu + Ce) result in different properties of colloid particles of cerium and copper citrates [26], leading to different behavior of decomposition and crystallization of the citrates, thus effecting adhesion stability of the active components on the support, as analyzed in section 4.1. Under the conditions in this work, the favorable ratio of citric acid/(Cu + Ce) is 1. High heating rate of the

dipped monolith leads to poor adhesion stability, which may be due to uneven temperature in the monolith. When calcination is carried out at high heating rate, the temperature of the catalyst precursor should increase much rapidly than that of the support, because the catalyst precursor is on the out surface of the monolith. The decomposition of metal citrates will start at about 280 °C (figure 3), while the temperature of the support is much lower than 280 °C at high heating rate. The formation of chemical bond between CeO_2, CuO nuclei produced from metal citrates decomposition and alumina on the surface of the support is difficult when the temperature of the support is at a low level, thus leading to poorer adhesion stability. This is consistent with adhesion analysis of section 4.1, in which an important step is to insert the hot FeCrAl support at 600 °C into the citrate sol.

The temperature of preheating FeCrAl support and calcination is fixed at 550 °C or 600 °C, because it was reported that $CuO–CeO_2$ catalysts show best performance when calcined at 500-650 °C. Higher temperature results in sintering the components, and lower temperature is unfavorable to highly disperse copper oxide and form interaction between the copper oxide and cerium oxide [2,4,7,8,25].

5. Conclusions

The present work shows that good adhesion $CuO–CeO_2/Al_2O_3$/FeCrAl monolithic catalysts can be prepared by the sol-pyrolysis method. High surface energy of the small crystal nuclei and the interaction between the active components and the support promote the adhesion stability. The presence of the FeCrAl support results in the decrease of CeO_2 particle size and aggregation of some CuO component. The $CuO–CeO_2/Al_2O_3$/FeCrAl monolithic catalysts exhibit very good catalytic performance for PROX, indicating that they are promising for the preferential oxidation of carbon monoxide in the reforming gases.

Acknowledgments

The authors would like to acknowledge National Natural Science Foundation of China (Granted as No. 20476079) and Hi-tech Research and Development Program of China (Granted as No. 2006AA05Z115) for funding of this research.

References

[1] O. Goerke, P. Pfeifer and K. Schubert, Appl. Catal. A Gen. 263 (2004) 11.
[2] G. Avgouropoulos, T. Ioannides and H. Matralis, Appl. Catal. B Environ. 56 (2005) 87.
[3] Y. Liu, Q. Fu and M.F. Stephanopoulos, Catal. Today 93 (2004) 241.
[4] G. Avgouropoulos, T. Ioannides, H.K. Matralis, J. Batista and S. Hocevar, Catal. Lett. 73 (2001) 33.
[5] G. Marba'n and A.B. Fuertes, Appl. Catal. B Environ. 57 (2005) 43.
[6] M. Watanabe, H. Uchida, K. Ohkubo and H. Igarashi, Appl. Catal. B Environ. 46 (2003) 595.
[7] F. Marino, C. Descorme and D. Duprez, Appl. Catal. B Environ. 58 (2005) 175.
[8] G. Avgouropoulos and T. Ioannides, Appl. Catal. A Gen. 244 (2003) 155.
[9] P.K. Cheekatamarla, W.S. Epling and A.M. Lane, J. Power Sources 147 (2005) 178.
[10] G.W. Roberts, P. Chin, X.L. Sun and J.J. Spivey, Appl. Catal. B Environ. 46 (2003) 601.
[11] S. Srinivas, A. Dhingra, H. Im and E. Gulari, Appl. Catal. A Gen. 274 (2004) 285.
[12] G.W. Chen, Q. Yuan, H.Q. Li and S.L. Li, Chem. Eng. J. 101 (2004) 101.
[13] L.A. Isupova, G.M. Alikina, O.I. Snegurenko, V.A. Sadykov and S.V. Tsybulya, Appl. Catal. B Environ. 21 (1999) 171.
[14] T. Suetsuna, S. Suenaga and T. Fukasawa, Appl. Catal. A Gen. 276 (2004) 275.
[15] A.D. Qi, S.D. Wang, G.Z. Fu, C.J. Ni and D.Y. Wu, Appl. Catal. A Gen. 281 (2005) 233.
[16] E. Tronconi, G. Groppi, T. Boger and A. Heibel, Chem. Eng. Sci. 59 (2004) 4941.
[17] B. Lindström, J. Agrell and L.J. Pettersson, Chem. Eng. J. 93 (2003) 91.
[18] T. Vergunst, F. Kapteijn and J.A. Moulijn, Appl. Catal. A Gen. 213 (2001) 179.
[19] X. Ouyang and R.S. Besser, J. Power Sources 141 (2005) 39.
[20] X.D. Wu, D. Weng, S. Zhao and W. Chen, Surf. Coat. Technol. 190 (2005) 434.
[21] M. Valentini, G. Groppi, C. Cristiani, M. Levi, E. Tronconi and P. Forzatti, Catal. Today 69 (2001) 307.
[22] F.X. Yin, S.F. Ji, N.Z. Chen, M.L. Zhang, L.P. Zhao, C.Y. Li and H. Liu, Catal. Today 105 (2005) 372.
[23] H.S. Li and J.F. Wang, Chem. Eng. Sci. 59 (2004) 4861.
[24] W. Wang, H.B. Zhang, G.D. Lin and Z.T. Xiong, Appl. Catal. B Environ. 24 (2003) 219.
[25] S.H. Zeng, B. Xue, X.Y. Wang, W.G. Yu and Y. Liu, J. Rare Earths. 24 (2006) 177.
[26] W.X. Kuang, Y.N. Fan, K.W. Yao and Y. Chen, J. Solid State Chem. 140 (1998) 354.